Functional Evaluation of Normothermic Ischemia and Reperfusion Injury in Dog Kidney by Combining MR Diffusion-Weighted Imaging and Gd-DTPA Enhanced First-Pass Perfusion

Ai-Shi Liu, MD* and Jing-Xia Xie, MD

Purpose: To evaluate functional alterations of renal ischemia and reperfusion injury using MR diffusion-weighted imaging and dynamic perfusion imaging.

Materials and Methods: Twelve dogs were randomly divided into four groups. Animal renal ischemia was respectively induced for 30 (group 1), 60 (group 2), 90 (group 3), and 120 (group 4) minutes by left renal artery ligation under anesthesia. Using a 1.5 T MR system, true-FISP, TSE, EPI, and DWI sequences were acquired in five different periods; specifically, pre-ischemia, onset-ischemia, late ischemia, onset-reperfusion, and post-reperfusion. Moreover, a turbo-FLASH sequence (TR/TE/TI/FA = 5.8/3.2/400 msec/10°) with a temporal resolution of 1.16 seconds was acquired. Signal intensity (SI) was measured in the cortex, outer medulla, and inner medulla of kidney. Apparent diffusion coefficient (ADC) values were calculated, and SI was plotted as a function of time.

Results: In all animals, significant SI changes of the left kidney on T2/T2*WI were detected following ischemia-reperfusion insult compared to corresponding values of the right kidney. Following ligation, the ADC values decreased in all layers of the left kidney. Immediately after the release of ligation, ADC values in both outer and inner medulla of the left kidney remained lower than those of the right kidney in those animals which were induced with renal ischemia for 60, 90, and 120 minutes. In all groups, a uniphasic enhancement pattern was observed in the outer and inner medulla of the left kidney, accompanied by a decrease of the area under the curve.

Conclusion: Our results suggest that MR diffusion-weighted imaging and dynamic perfusion imaging are useful in identifying renal dysfunction following normothermic ischemia and reperfusion injury.

Key Words: fMRI: functional magnetic resonance imaging; kidney; DWI: diffusion-weighted imaging; ischemia; perfusion; dog

J. Magn. Reson. Imaging 2003;17:683–693. © 2003 Wiley-Liss, Inc.

Department of Radiology, Peking University Third Hospital, Beijing, Peoples Republic of China

*Address reprint requests to: to A-S.L., Dept. of Radiology, Peking University Third Hospital, 49 North Garden Road, Haidian District, Beijing 100083, P.R. China. E-mail: liuaishi2000@yahoo.com

Received October 23, 2002; Accepted January 28, 2003

DOI 10.1002/jmri.10312

Published online in Wiley InterScience (www.interscience.wiley.com).

AFTER RENAL TRANSPLANTATION, acute tubular necrosis (ATN) caused by prolonged ischemia and reperfusion injury is traditionally one of the most common causes of delayed graft function. Until now, color Doppler sonography and radionuclide imaging techniques have been used for evaluating renal graft dysfunction. However, Doppler sonography, often used for the evaluation of early vascular complications, is of limited value in assessing renal function. Moreover, radionuclide study is unable to discriminate between the cortex and medulla, which restricts its application in morphologic evaluation. In addition, no clinical or laboratory parameters to monitor graft dysfunction in patients with ATN are presently available. Therefore, a needle core biopsy is required for histopathologic assessment of renal transplant, at increased risk (1-3).

Magnetic resonance imaging is the first diagnostic method allowing high spatial resolution imaging of renal morphology as well as quantitative evaluation of renal function. The kidney is particularly amenable to functional imaging study, due to its high blood flow and water transport functions. Functional magnetic resonance imaging (fMRI) of the kidney with fast imaging techniques is currently employed in both basic studies and clinical applications, and provides novel insights into renal physiology and pathophysiology (4-5). The use of fast imaging techniques is very promising for the evaluation of diffusion and perfusion in both healthy and diseased kidneys. MR diffusion-weighted imaging (DWI) is currently the only method available to assess molecular diffusion in vivo in a noninvasive fashion. In vivo measurement of the apparent diffusion coefficient (ADC) provides a means to explore the functional status of the kidney (6-12). In addition, contrast-enhanced MR techniques have been described previously (13–25). After the administration of paramagnetic agents (i.e., Gd-DTPA), followed by dynamic MR imaging with high temporal resolution, the first pass of the MR contrast agent is monitored. Meanwhile, signal intensity-time (SI-T) curves in various zones of kidneys are acquired, which reveal differences between well-functioning and pathologic kidneys over time. To date, no renal complications have been reported from the clinical use of Gd-DTPA injections (26). To our knowledge, very few studies have examined the use of a combination of MR

diffusion and perfusion imaging to assess renal function (10).

The purpose of this study was to investigate the feasibility of using MR T2/T2*-weighted imaging, diffusion-weighted imaging and Gd-DTPA enhanced first-pass perfusion for the evaluation and monitoring of alterations in renal function following normothermic ischemia and reperfusion injury in dog kidney in vivo.

MATERIALS AND METHODS

Experimental Animals

A total of 12 mixed-breed male dogs with a mean body weight of 16.8 kg (range: 13.0 to 24.1 kg) were consecutively studied. Animals were allocated in a random fashion to one of the four groups, based on the duration of ischemia. Food was withheld 12 hours prior to surgical procedures. Each animal was anesthetized by the intravenous administration of Phenobarbital sodium (30 mg/kg). Dogs breathed spontaneously during all experiments. A flank incision was made on the left upper side of the abdomen in each animal. During surgery, considerable attention was paid to all the branches of the left artery separated near the renal hilum in order that the main renal artery was patent and free from damage. The left artery was loosely coiled using a plastic string for subsequent ligation. A cannula was advanced into the left ureter for urine collection, in order to measure urinary protein (Up) before and after ischemia-reperfusion injury. The left femoral vein was cannulated via incision at the left femoral triangle for the administration of additional anesthesia and paramagnetic contrast agent for blood sampling to determine serum creatinine levels. Serum creatinine (sCr) was used as an index of renal function before and after insult. The right kidney, which served as a control, was not manipulated. The left kidneys of animals in groups 1 to 4 were subjected to normothermic ischemia for 30, 60, 90, and 120 minutes, respectively, via ligation of the left renal artery using plastic string, followed by reperfusion injury for 1 hour with the release of occlusion. Following the completion of experiments, dogs were euthanatized using an overdose of phenobarbital. Both kidneys were removed immediately, and renal tissues, including the cortex, outer medulla, and inner medulla, were examined by light microscopy and transmission electron microscopy (JEM-100 CX II, JOEL Ltd., Tokyo, Japan). Kidneys were sectioned into 3-mm slices, fixed in isotonic buffered 10% formalin, and examined by light microscopy after standard hematoxylin-eosin staining. One pathologist, who was blinded to the procedure of vascular ligation, reviewed histological findings. This experiment was performed in accordance with the Guide for the Care and Use of Laboratory Animals, with the approval of the Beijing Municipal Science and Technology Committee.

MR Imaging

Each animal was placed in the supine position and underwent MR imaging on a commercially available 1.5-T MR imager (Siemens Magnetom Vision, Erlangen, Germany). A head coil was used to obtain all the se-

of time.

quences in the present study. Before ligation of the left renal artery, the true fast imaging with steady-state precession (true-FISP) sequence (TR/TE = 4.8/2.3msec, flip angle = 70°) was initially acquired to determine the optimal midcoronal planes of the bilateral kidneys. Next, T1-weighted FLASH (fast low-angle shot) $(TR/TE = 122/4.1 \text{ msec}, \text{ flip angle} = 80^\circ) \text{ and } T2$ weighted TSE (turbo spin-echo) (5000/138 msec [repetition time/effective echo time]; echo train length, 29) sequences of the axial section of both kidneys were acquired with a matrix of $114-140 \times 256$, field of view (FOV) = 225×300 mm, and section thickness of 5 mm with an intersection gap of 1 mm. One signal was acquired. Following routine T1- and T2-weighted imaging, diffusion-weighted imaging was performed using a diffusion-weighted multislice spin-echo type sequence that combined a diffusion-sensitizing gradient (DSG) before and after the 180° pulse with an echo-planar imaging (EPI) read-out. Fat suppression was performed to avoid severe chemical artifacts. Diffusion-weighted EPI with a TE of 123 msec were obtained along the transverse plane, with the DSG oriented in the cephalocaudal direction. Other imaging parameters employed include: 128×128 matrix, FOV = 230×230 mm, section thickness = 5 mm, and 1 excitation. The ADC value for serial diffusion-weighted EPI sequences was calculated using the formula: ADC =-ln $(S/S_0)/(b$ b₀), where S₀ and S are signal intensities in regions of interest (ROI), including cortex (C), outer medulla (OM), and inner medulla (IM), obtained with three different gradient factors ($b_0 = 0$, b = 30, and 300 seconds/mm², respectively). Three ADC values were obtained when the above b-values were combined. The mean of these three values was calculated. ROI were positioned on the renal parenchyma at the same level of the upper pole and central portion of the bilateral kidneys, avoiding major vascular structures, artifacts such as chemical shift, and magnetic susceptibility artifacts. All the abovementioned sequences were obtained repeatedly, with no changes in respective imaging parameters after onset-ischemia (just after arterial occlusion), late-ischemia (just before the release of arterial occlusion), onset-reperfusion (immediately after the release of arterial occlusion), and post-reperfusion (1 hour after the release of arterial occlusion) (Fig. 1). Finally, inversionrecovery 2-D turbo-FLASH (TR/TE/TI/FA = 5.8/3.2/ 400 msec/10°) was used to monitor the first pass of Gd-DTPA (Magnevist, Schering, Berlin, Germany) through renal parenchyma with a matrix of 112×128 , FOV = 263×300 mm, resulting in a temporal resolution of 1.16 seconds. After the fifth image was obtained, a bolus of Gd-DTPA (0.1 mmol/kg) was rapidly administered with an automatic MR power injector (Spectris, SMR200, Medrad Inc., Pittsburgh, PA) at a flow rate of 3 mL/seconds, followed by a 10-mL saline flush at the same rate. A hundred slices were obtained at the same level of the bilateral kidneys with no inter-image delay. Four circular nonoverlapping ROI measuring 0.1-0.2 cm² (i.e., a diameter of 2–3 mm) were selected from the cortex, outer medulla, and inner medulla. Mean signal intensity (SI) measurements were obtained for all ROI at the same location. SI results were plotted as a function

fMRI in Dog Kidney 685

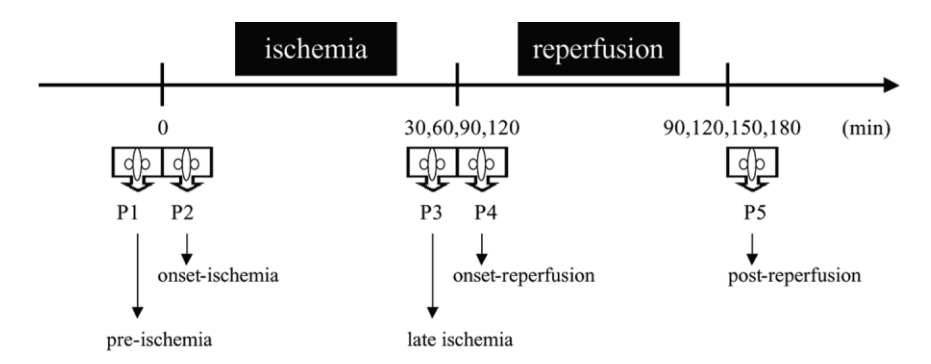


Figure 1. MR imaging protocol illustrated that T2/T2*WI and DWI were performed in five different periods, specifically, pre-ischemia (PI), onset-ischemia (P2), late ischemia (P3), onset-reperfusion (P4) and post-reperfusion (P5) during this experimental study.

Statistical Analysis

With the use of standard image analysis software available on the MR unit, renal SI was analyzed before and after left arterial ligation, and after the removal of ligation on true-FISP, TSE, and the diffusion-weighted EPI series in the different layers (C, OM, and IM) of both kidneys in each group. The ADC values of the upper pole and central portion were calculated. Mean ADC values in the different layers of bilateral kidneys were compared between left and right kidneys. For quantitative assessment of renal Gd-DTPA kinetics on the timecourse curves, peak height (P), time to peak (Tp), and the area (A) under the time-course curves after intravenous injection of Gd-DTPA were estimated. Some measurements of signal intensity values by automatic image propagation were not performed due to misregistration.

All values were expressed as mean \pm SD. Data analyses were performed on a personal computer using the SPSS program package. The paired Student's t-test was used to compare the differences within each group. Analysis of variance (ANOVA) test was employed to compare the differences between groups. A value of P < 0.05 was considered statistically significant.

RESULTS

SI Changes on T2/T2*WI

T2/T2*-weighted images revealed three different layers of the kidney, consistent with the macroscopic appear-

ance of resected specimens (Fig. 2). Before artery ligation, no significant differences were noted in the SI of each layer of both kidneys on true-FISP, TSE, and EPI. After the onset of ligation, there was a markedly significant reduction in the SI of each layer of the left kidney compared to the right kidney, except for the SI of the inner medulla on the TSE image (Table 1). After the removal of ligation, no significant differences were noted between the SI of the cortex in the left and right kidneys. However, in all the groups, the SI of outer and inner medulla of the left kidney on true-FISP and EPI remained significantly lower than that of the right kidney, in particular, signal changes of the outer medulla on EPI (Table 2, Fig. 3).

ADC Values Changes

The ADC values of the different layers of bilateral kidneys in the five conditions are presented in Table 3. Before ligation, no significant differences were observed in the ADC values of individual layers of both kidneys. After ligation, the values decreased in all left renal parenchyma layers, with the most pronounced changes in the cortex and outer medulla. Immediately after the removal of ligation, ADC values in the cortex of the left kidney increased, and levels were equivalent in both renal cortices. However, in all groups, ADC values in both outer and inner medulla of the right kidney remained higher than those of the left kidney. After reperfusion injury, ADC values in both outer and inner medula of the right with the respective of the left kidney.

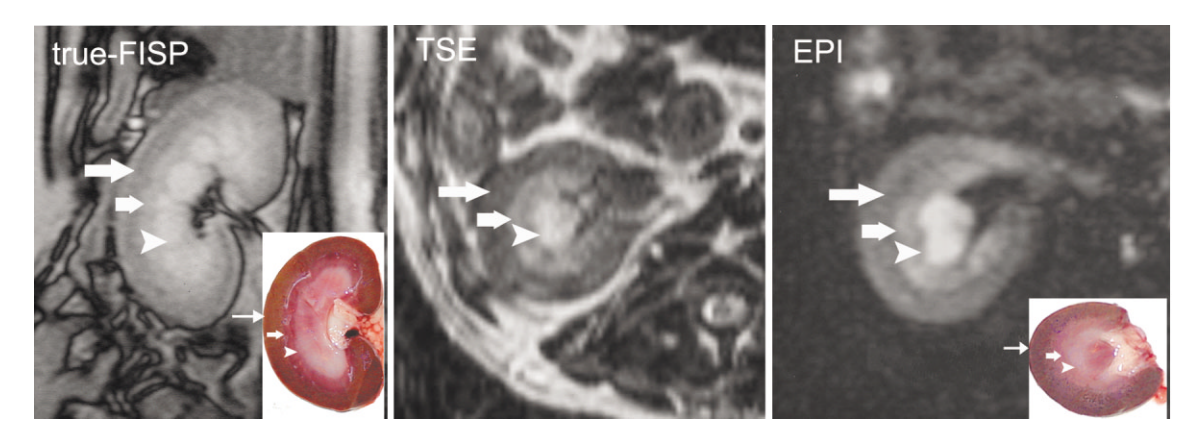


Figure 2. T2/T2*-weighted images and resected specimens of the normal canine kidney clearly reveal three different layers of kidneys: C (long arrows), OM (short arrows), and IM (arrowheads).

Table 1
Comparisons of Mean Signal Intensity (SI) Between Pre- and Post-Ligation in True-FISP, TSE and EPI Sequences

Laurana	Pre-ligatio	n (N = 12)	Post-ligation	n (N = 12)
Layers	RK	LK	RK	LK
True-FISP				
С	774.4 ± 102.1	736.2 ± 148.3	740.1 ± 92.2	569.4 ± 89.8^{b}
OM	964.5 ± 98.4	922.8 ± 165.3	942.9 ± 100.4	660.1 ± 116.3 ^b
IM	1217.2 ± 153.3	1176.5 ± 206.6	1220.7 ± 149.5	968.7 ± 178.5^{a}
TSE				
С	626.0 ± 42.7	634.8 ± 121.8	589.1 ± 123.7	347.4 ± 102.0^{b}
OM	804.7 ± 86.7	829.2 ± 145.1	777.5 ± 109.4	504.0 ± 146.3^{b}
IM	1025.7 ± 109.8	1018.0 ± 96.4	981.2 ± 81.3	968.3 ± 172.6
EPI				
С	468.8 ± 119.7	470.2 ± 128.0	442.3 ± 82.7	156.6 ± 43.26 ^b
OM	655.7 ± 132.1	656.8 ± 151.7	622.0 ± 138.2	363.1 ± 159.4 ^b
IM	1059.6 ± 164.9	994.5 ± 181.6	1075.3 ± 247.7	786.3 ± 181.0^{b}

aP < 0.01.

FISP = fast imaging with steady-state precession, TSE = turbo spin-echo, EPI = echo planar imaging (b = 0), RK = right kidney, LK = left kidney, C = cortex, OM = outer medulla, IM = inner medulla.

dulla of the left kidney remained lower than those of the right kidney in groups 2, 3, and 4. DWI revealed different appearances of bilateral kidneys during the ischemia-reperfusion injury (Fig. 4).

Renal Perfusion Changes

Dynamic turbo-FLASH images clearly depicted Gd-DTPA transit through the kidneys as three phases of centripetal migration of the high-signal band from the C to the IM layer. In our experiment, dynamic Gd-enhanced perfusion imaging demonstrated that the SI-T curve also comprised three phases in the cortex, outer medulla, and inner medulla of the right kidney. After a bolus injection of Gd-DTPA, there was an initial sharp increase (first or vascular phase) in cortical signal intensity within the first 11 seconds corresponding to migration of the contrast agent through the interlobular arteries and glomerular capillary networks, followed by a slight decrease in signal intensity due to washout of the agent. A second peak (second or tubular phase) corresponded mainly to the appearance of the contrast agent in the proximal convoluted tubule. This was followed by a slow gradual increase (third phase), which was maintained for the remaining investigation time, corresponding mainly to the appearance of the contrast agent in the distal convolutes and recirculated agent. The three phases in the outer medulla resembled those in the cortex. At about 14 seconds after administration of the contrast agent, the first peak was observed in the outer medulla, possibly reflecting the migration of the contrast agent through long peritubular capillary beds. The second peak corresponded mainly to the appearance of the contrast agent in the proximal convoluted tubule, and the third phase of the outer medulla was similar to that of the cortex. The first peak of the inner medulla corresponding to the movement of the contrast agent through capillary beds around the loop of Henle was minimal or even unclear, whereas the second peak corresponding mainly to the appearance of the contrast agent in the loop of Henle was evident. This high-signal band may represent the Gd-DTPA concentration in the loop of Henle. The third phase of the inner medulla

corresponded to the presence of the contrast agent in the collecting ducts, possibly representing the Gd-DTPA concentration within the collecting ducts.

In contrast, there were markedly different enhancement curves between each layer of the right and left kidneys among the groups. The first peak of the left renal cortex diminished in both groups 1 and 2, whereas it appeared as a plateau in groups 3 and 4, which implied the filtration rate of the contrast agent decreased with the prolongation of ischemia. The second peak of the left renal cortex disappeared in all groups following ischemia-reperfusion injury. After reperfusion, contrast-enhanced MR images of the left kidney revealed a uniphasic enhancement pattern in OM and IM compared to those of the right kidney. In all groups, the first and second peak was not observed in both OM and IM (Figs. 5, 6). Time-to-peak (Tp) of the left renal cortex was universally delayed by 2-3 seconds compared to the right kidney, without any significant differences in peak height (P). The area under the curve of the left kidney remained similar to that of the right kidney in the cortical layer of most groups except group 1. Neither P nor Tp in the outer medulla of the left kidney were identified on SI-T curves, and the area under the curve was significantly less than that of the right kidney in each group. The area under the curve of the inner medulla of the left kidney was significantly less than that of the right kidney in all groups (Table 4).

Serum Creatinine (sCr) and Urinary Protein (Up)

There were no major differences between the sCr levels in pre-ischemia and post-reperfusion in all animals. Up was qualitatively determined in all dogs before ischemia and after reperfusion injury. There were no significant differences in Up values for all animals between groups before ischemia (P=.678). In contrast, following reperfusion injury, a dramatically increased Up value was detected between groups (P=.002). Up gradually increased with the prolongation of ischemia, implying the accelerative damage of renal function following hypoxemia (Fig. 7).

 $^{^{}b}P < 0.001.$

0), RK = right kidney, LK = left kidney, C = cortex, OM = corter medulla, IM = inner medulla.

= fast imaging with steady-state precession, TSE = turbo spin-echo, EPI = echo planar imaging (b =

Comparisons of Mean Signal Intensity (SI) After the Removal of Ligation in True-FISP, TSE and EPI Sequences Between Left and Right Kidneys

0,000	Group 1 $(N=3)$	(N=3)	Group 2	Group 2 ($N=3$)	Group 3 $(N = 3)$	(N=3)	Group 4 ($N = 3$)	(N=3)
Layers	杀	LK	¥	LK	Ж	LK	꿆	¥
True-FISP								
O	793.9 ± 130.6	754.8 ± 108.2	772.5 ± 77.1	706.1 ± 25.1	703.1 ± 132.3	685.1 ± 41.8	650.1 ± 127.5	600.2 ± 90.6
MO	985.8 ± 83.3	888.8 ± 104.4^{a}	1009.7 ± 78.7	850.2 ± 106.1^{a}	1030.0 ± 91.1	849.6 ± 107.4^{a}	874.4 ± 233.3	657.3 ± 156.7^{a}
≥	1187.8 ± 109.2	1169.3 ± 141.5	1186.9 ± 132.5	994.8 ± 126.7^{a}	1190.8 \pm 165.6	792.8 ± 95.9^{a}	1117.5 \pm 292.3	912.4 ± 194.3^{a}
TSE								
O	550.6 ± 270.3	509.2 ± 324.7	594.6 ± 36.0	689.0 ± 130.4	603.1 ± 51.3	596.7 ± 23.3	522.6 ± 31.6	590.6 ± 11.3
MO	660.1 ± 234.3	577.8 ± 329.9	751.2 ± 23.3	854.2 ± 157.0	805.4 ± 70.2	685.1 ± 46.1	675.6 ± 46.8	708.0 ± 18.4
≥	815.0 ± 168.4	797.6 ± 241.9	918.2 ± 55.7	1103.4 \pm 202.2	1107.7 ± 110.7	979.2 ± 97.9	993.3 ± 27.5	1022.3 ± 25.5
EPI								
O	481.7 ± 62.9	415.1 ± 58.3	418.2 ± 40.8	402.7 ± 78.1	382.3 ± 32.7	315.3 ± 44.0	518.0 ± 99.7	438.5 ± 163.3
MO	599.8 ± 81.4	364.4 ± 43.5^{b}	596.0 ± 70.8	419.7 ± 50.5^{b}	563.9 ± 37.7	404.6 ± 62.6^{b}	732.5 ± 68.4	386.8 ± 34.5^{b}
⅀	1163.6 ± 114.8	$678.8 \pm 68.2^{\rm b}$	978.3 ± 85.8	$656.7 \pm 60.5^{\mathrm{b}}$	1009.3 ± 92.4	676.9 ± 48.5^{a}	1096.6 ± 135.4	620.0 ± 30.3^{a}
$^{\mathrm{a}}P < 0.05.$								
$^{ m b} {\cal P} < 0.01.$								

Pathologic Changes

Glomeruli had normal cellularity with patent glomerular capillaries. In groups 1 and 2, endothelial cells in the proximal and distal tubules of the left kidney suffered no fundamental lesions, despite general edema. In contrast, the proximal and distal tubules of the left kidney in groups 3 and 4 displayed profound tubular endothelial changes, such as cloudy swelling of epithelial cells, intratubular denuded epithelium and cellular debris, and regional necrosis of tubular cells. The tubular lumina contained protein casts. Hemorrhage was observed in the interstitium and renal tubules (Fig. 8). Diffuse mitochondrial vacuolization of endothelial cell was noted in the majority of convoluted and straight proximal tubules.

DISCUSSION

This preliminary study reveals morphologic and functional changes in different layers of bilateral kidneys on T2/T2*WI, DWI, and perfusion imaging in different time periods of normothemic ischemia and reperfusion injury. In particular, compared to the right kidney control, significant changes were observed in the OM and IM of the left kidney, in correlation with pathologic findings.

In our experiments, the OM layer of the left kidney was most severely damaged. After the onset of left renal arterial ligation, deoxyhemoglobin accumulated in the renal parenchyma, because blood inflow ceased. Oxyhemoglobin is diamaganetic, whereas deoxyhemoglobin is paramagnetic. As a result, SI on T2/T2*WI of each layer of the left kidney in all groups markedly decreased, except TSE images of the IM layer. After arterial occlusion, SI on EPI of the left kidney significantly decreased, which was in agreement with a previous study (27). During reperfusion, SI in the cortex of the left kidney was almost restored to pre-ligation levels similar to that of the right kidney. It is most likely that oxyhemoglobin replaced deoxyhemoglobin in glomerular capillaries after arterial release. However, in the OM and IM layers of the left kidney, SI on true-FISP and EPI remained lower than those of the right kidney, except true-FISP images of the IM layer of the left kidney in group 1. These findings could relate with severe hemorrhage in the interstitium and renal tubules. EPI was possibly more sensitive to magnetic field inhomogeneity than true-FISP. In addition, the IM layer of the left kidney in group 1 may have been slightly damaged.

In EPI diffusion imaging, the ADC values of the kidney were much higher than that of water at body temperature, which may be attributed to other factors, such as capillary perfusion, tubular flow, and water content (6,8,11,28). In previous studies using small b-values, the ADC values reflect effects from both perfusion and diffusion. However, when larger b-values (greater than 500 seconds/mm²) are used for renal diffusion-weighted imaging, the signals of the kidneys are markedly diminished, because the ADC of renal tissue is higher than that of any other organs in the abdomen (11). Therefore, small and middle b-values were selected in this study. Immediately after the onset of ligation and during ischemia, the ADC values of the

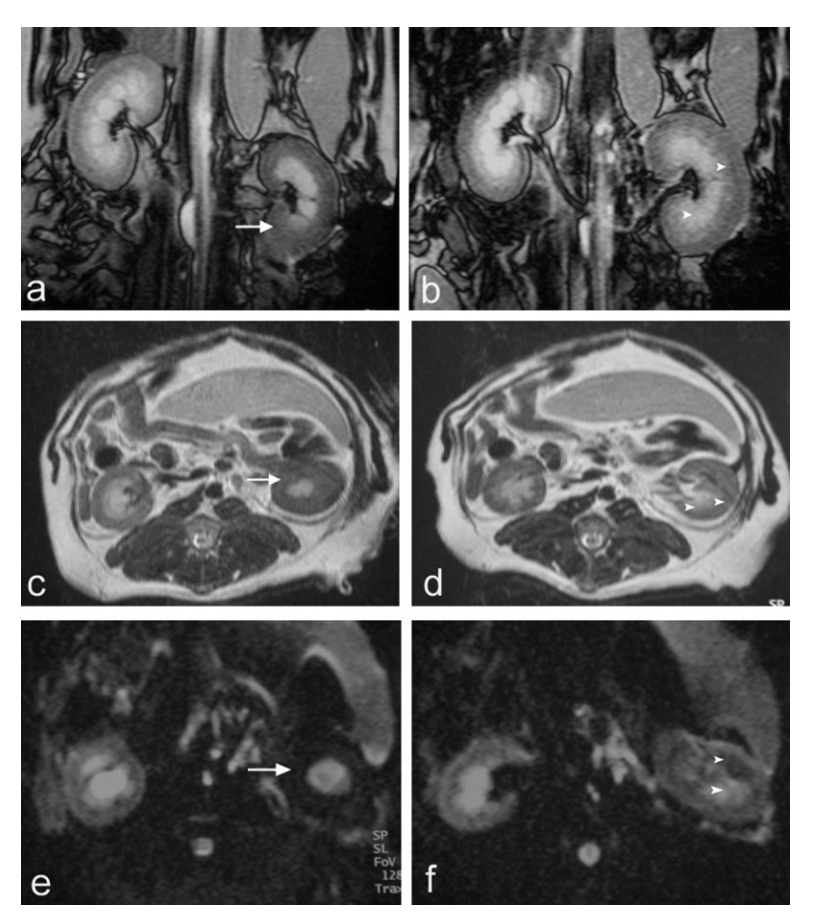


Figure 3. T2/T2*-weighted images on true-FISP (**a, b**), TSE (**c, d**), and EPI (**e, f**) from an animal in group 3. SI values in C, OM, and IM of the left kidney markedly decreased after renal artery ligation (arrow) (a, e). Compared to the right kidney, SI values in OM and IM of the left kidney remained lower after the release of ligation (arrowheads) (b, f). SI values in C and OM of the left kidney decreased after renal artery ligation (arrow) (c); SI values in C and OM of the left kidney increased after the release of ligation (arrowheads) (d).

left renal cortex diminished in each group. However, after the release of ligation, the ADC values of the left renal cortex increased to a value similar to that of the right kidney. In the reperfusion phase, although the

ADC values of the cortex of the left kidney were lower than those of the right kidney, the differences were not significant (P > .05 in each group). In our experiments, the ADC values of the cortex reflected contribution to

Table 3
Comparisons of ADC Values (×10⁻³ mm²/second) in Different Layers in Five Conditions Between Left and Right Kidneys

Lovers	Group 1	(N = 3)	Group 2	2(N = 3)	Group 3	8 (N = 3)	Group 4	1 (N = 3)
Layers	RK	LK	RK	LK	RK	LK	RK	LK
Pre-ischemia								
С	3.64 ± 0.78	3.25 ± 0.66	3.30 ± 0.70	2.76 ± 0.53	3.32 ± 1.22	2.84 ± 1.11	3.23 ± 0.72	3.08 ± 0.57
OM	3.08 ± 0.50	2.75 ± 0.32	2.76 ± 0.87	2.60 ± 0.65	3.05 ± 0.76	2.60 ± 0.75	2.51 ± 0.44	2.85 ± 0.89
IM	3.21 ± 0.51	2.84 ± 0.25	2.80 ± 0.58	2.52 ± 0.33	3.14 ± 0.96	2.62 ± 0.88	2.83 ± 0.77	2.88 ± 0.67
Onset-ischemia								
С	3.35 ± 0.38	2.31 ± 0.71^{a}	3.53 ± 0.51	1.69 ± 0.26^{b}	3.35 ± 0.95	2.12 ± 0.45^{a}	3.70 ± 0.98	1.95 ± 0.54^{a}
OM	2.64 ± 0.47	1.91 ± 0.28^{a}	3.07 ± 0.82	1.78 ± 0.49^{b}	3.33 ± 0.86	1.69 ± 0.59^{a}	3.03 ± 0.68	2.07 ± 0.28^{a}
IM	2.74 ± 0.59	1.92 ± 0.29^{a}	2.46 ± 0.57	1.54 ± 0.53^{a}	2.73 ± 0.88	1.70 ± 0.29^{a}	2.96 ± 0.74	2.01 ± 0.55^{a}
Late ischemia								
С	3.43 ± 0.92	1.68 ± 0.77^{a}	3.43 ± 0.84	1.73 ± 0.42^{b}	3.52 ± 1.56	2.05 ± 0.75^{a}	3.53 ± 0.92	1.30 ± 0.32^{b}
OM	3.31 ± 0.61	2.13 ± 0.28^{b}	3.57 ± 0.75	2.21 ± 1.16 ^a	3.08 ± 0.98	1.82 ± 0.40^{a}	3.23 ± 1.32	1.57 ± 0.59^{a}
IM	2.94 ± 0.62	2.23 ± 0.46^{a}	3.16 ± 0.30	1.80 ± 0.74^{b}	2.80 ± 0.96	1.55 ± 0.24^{a}	3.27 ± 1.01	2.32 ± 0.82^{a}
Onset-reperfusion								
C	3.57 ± 0.75	3.06 ± 0.87	3.60 ± 1.17	3.12 ± 0.36	3.31 ± 1.20	2.88 ± 0.43	4.09 ± 1.26	3.18 ± 0.59
OM	3.64 ± 1.16	2.44 ± 0.92^{a}	2.71 ± 0.55	2.18 ± 0.32^{b}	3.20 ± 0.86	2.02 ± 0.36^{a}	3.32 ± 1.03	2.28 ± 0.90^{a}
IM	3.28 ± 0.62	1.18 ± 0.64^{a}	2.85 ± 0.48	1.93 ± 0.43^{b}	2.99 ± 0.99	1.79 ± 0.30^{a}	3.31 ± 0.93	2.45 ± 0.61^{a}
Post-reperfusion								
C	3.38 ± 0.57	3.02 ± 0.43	3.54 ± 1.07	3.36 ± 0.72	3.37 ± 0.96	2.62 ± 0.72	3.73 ± 0.81	3.00 ± 0.86^{a}
OM	3.37 ± 0.89	2.72 ± 0.73	2.94 ± 0.38	2.28 ± 0.24^{a}	2.96 ± 0.92	1.68 ± 0.46^{a}	3.25 ± 0.91	2.07 ± 0.70^{b}
IM	2.79 ± 0.45	2.67 ± 0.42	2.86 ± 0.41	2.04 ± 0.42^{a}	2.94 ± 1.01	1.79 ± 0.36^{a}	3.03 ± 0.97	2.34 ± 0.81^{a}

aP < 0.05.

 $^{^{}b}P < 0.01.$

fMRI in Dog Kidney 689

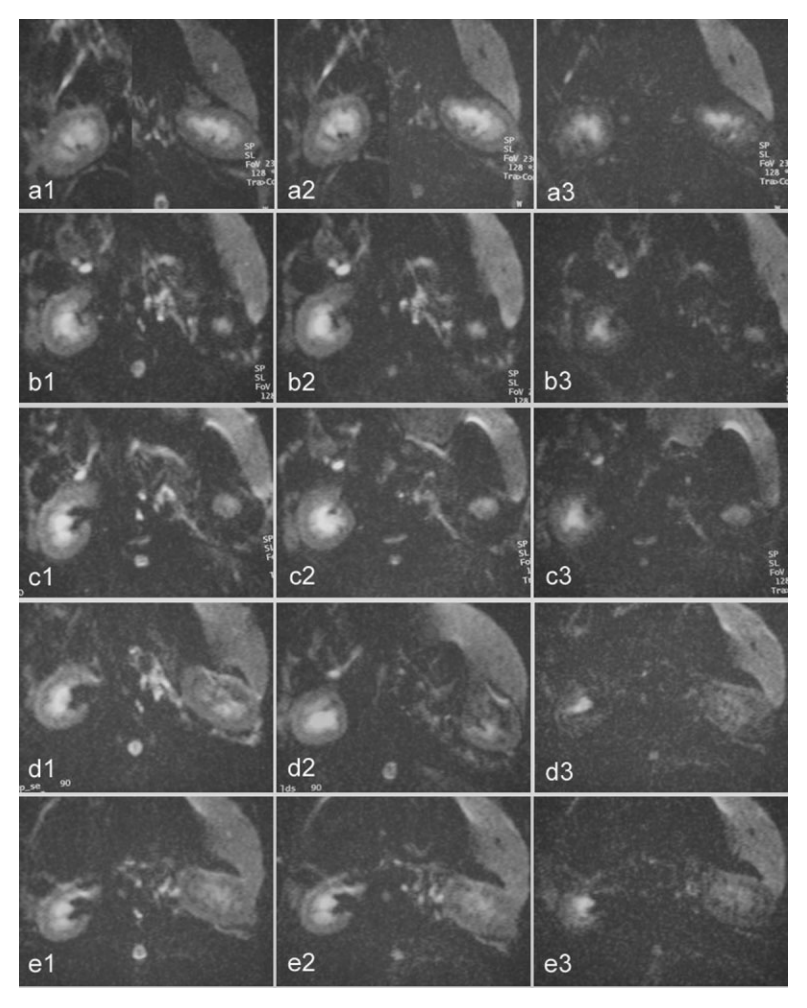


Figure 4. DW MR images on pre-ischemia (a1a3), onset-ischemia (b1-b3), late ischemia (c1c3), onset-reperfusion (d1-d3) and post-reperfusion (e1-e3) with b = 0 (left panel), b = 30 (middle panel), and b = 300 (right panel) were obtained from an animal in group 3. SI values in C, OM, and IM of the right kidney gradually decreased as b-value increased. SI values in OM and IM of the left kidney did not decrease significantly as the b-value increased during ischemia and reperfusion injury. After the arterial occlusion, hypointense band was evident in the cortex and outer medulla of the left kidney. Following the release of arterial occlusion, inhomogeneous hypointense was observed in the outer medulla of the left kidney.

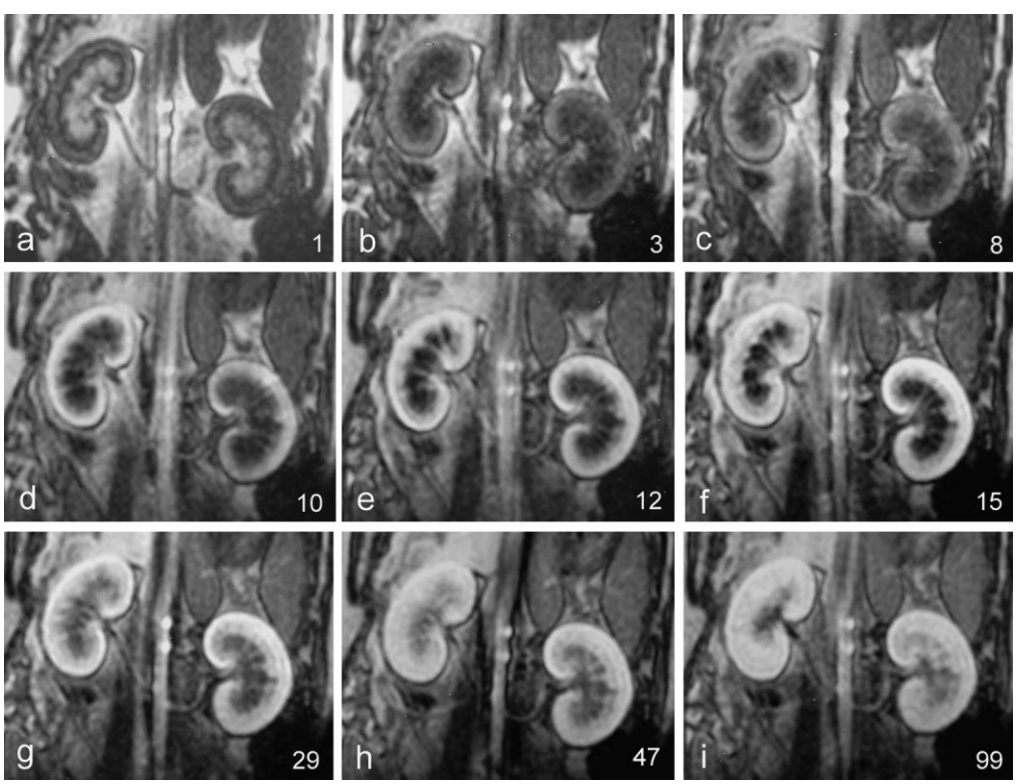


Figure 5. Gd-DTPA dynamic enhanced MR images from an animal in group 3 (**a-i**), depicting scans 1, 3, 8, 10, 12, 15, 29, 47, and 99, respectively. On images 29, 47, and 99, the signal intensity in OM and IM of the left kidney was persistently lower compared to that of the right kidney.

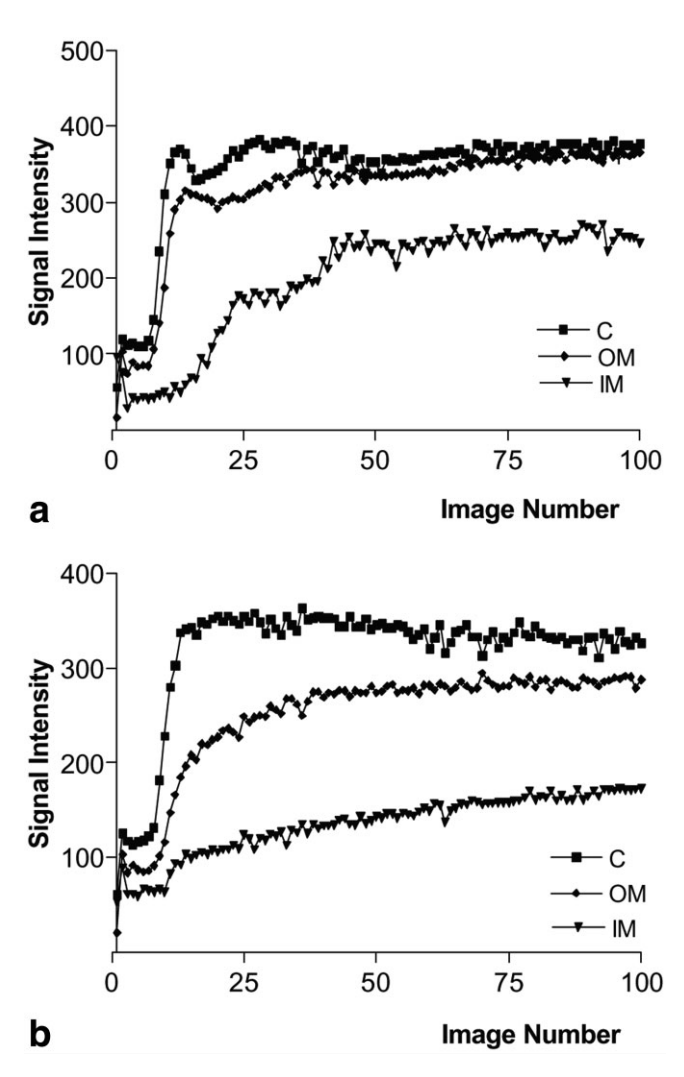


Figure 6. Time-course MR signal enhancement curves obtained from an animal in group 3. Three phases in each layer of the right kidney were clearly observed (a), whereas a uniphasic enhancement pattern in each layer of the left kidney was evident after ischemia-reperfusion injury (b).

blood perfusion, in agreement with previous results. In contrast, the ADC values of the OM and IM remained lower than those of the right kidney until post-reperfusion injury (except in group 1). One proposal to explain this finding is that the reduction of glomerular filtration rate, casts in the tubules, and edema of the tubular epithelial cells may participate in this complicated course, which led to diffusion-restriction. Following insult, OM and IM of the left kidney in groups 2, 3, and 4 were evidently damaged, which resulted in decrease or loss of the urinary concentration capacity of the renal tubule and collecting duct. There was no evidence of damage in the renal cortex (29–31). Medullary hypoxic injury is characterized by necrosis of tubules that are most remote from vessels; the renal medulla is most susceptible to anoxia (32). Marked anisotropic diffusion was observed within the renal medulla (8). The ADC values of the upper pole of kidneys were higher than those of the central portion with the DSG oriented in the cephalocaudal direction, because the tubules in the poles are parallel to DSG and the tubules in the mid polar region are horizontal to DSG (12). Our experi-

Comparisons of Peak Height, Time to Peak and Area Under the Curve on SI-T Curves Between Left and Right Kidneys

0,0,0	Group	Group 1 ($N = 3$)	Group 2 $(N=3)$	(N=3)	Group 3	Group 3 ($N = 3$)	Group 4 ($N=3$)	(N=3)
Layers	RK	놀	풒	LK	Æ	ᆂ	光	LK
O								
۵	392.3 ± 51.1	355.1 ± 9.8	307.8 ± 13.0	384.8 ± 55.9	377.0 ± 26.9	378.8 ± 33.2	375.6 ± 71.5	408.4 ± 48.4
T	10.9 ± 0.7	12.8 ± 1.3^{a}	11.2 ± 1.2	14.3 ± 1.3^{a}	11.2 ± 2.3	15.1 ± 1.3^{a}	10.1 ± 1.2	$13.2 \pm 1.3^{\rm a}$
⋖	41848.2 ± 1515.4	36486.1 ± 1311.8^{a}	36045.1 ± 1790.3	37072.4 ± 2317.8	43995.3 ± 2157.6	43408.2 ± 3730.7	49687.8 ± 3598.4	50965.8 ± 1760.0
MO								
۵	249.1 ± 6.0	Not identified	265.0 ± 15.6	Not identified	342.1 ± 41.6	Not identified	306.4 ± 10.1	Not identified
۲ª	12.8 ± 0.7	Not identified	13.9 ± 0.7	Not identified	14.3 ± 1.3	Not identified	13.9 ± 1.8	Not identified
`∢	38544.2 ± 3005.9	28978.3 ± 3949.8^{b}	32952.2 ± 3617.3	24665.2 ± 857.6^{a}	39349.1 ± 2298.9	$33708.7 \pm 2985.7^{\mathrm{a}}$	42478.1 ± 2624.2	37145.2 ± 4493.7^{a}
⅀								
∢	34313.4 ± 2827.6	22406.1 ± 1556.4^{b}	27111.5 ± 3407.0	21650.4 ± 1430.1^{a}	26104.1 ± 3510.3	20236.7 ± 3414.0^{a}	36871.4 ± 4038.0	26208.1 ± 2696.5^{b}
a 0 0 0 DE								

RK = right kidney, LK = left kidney, C = cortex, OM = outer medulla, IM = inner medulla, SI = signal intensity, P = peak height (first peak), T_p = time to peak (first peak) (unit: second), A = area under the curve (unit: mm^2) fMRI in Dog Kidney 691

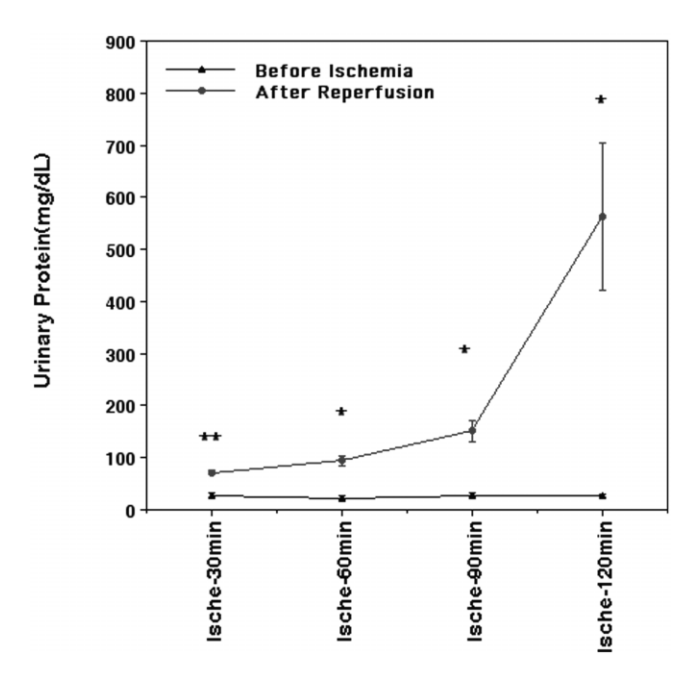


Figure 7. Level of animal urinary protein gradually increases with the prolongation of ischemia. Twelve dogs were randomly divided into four groups. Left renal ischemia was respectively induced for 30, 60, 90, and 120 minutes by occlusion of the left renal artery. Level of urinary protein of the animal was respectively measured before ischemia and after reperfusion. Data are mean \pm SD values (N=3). *P<0.05, **P<0.01 compared to values for level of urinary protein before ischemia by the paired Student's t-test.

ments revealed a large spread in data (Table 3), indicating substantial measurement error currently inherent to the technique. It is likely that anisotropic diffusion was not respected due to the small number of animals in each group, or that EPI is highly sensitive to motion and susceptibility, leading to signal loss and image distortion.

Dynamic MR images directly revealed renal morphology and indirectly reflected the functional status of renal vasculature, renal perfusion, and tubular concentrating ability. Following administration of Gd-DTPA, there were obviously different enhancement patterns in the different layers between the left and right kidney. Frank et al (33) defined three phases during the passage of the contrast agent through the kidney; specifically, vascular, tubular, and ductal phases, representing the outer cortex, outer medulla, and inner medulla, respectively. In this study, SI-T curves of the control kidney also comprised three phases in each layer, consistent with previously reported data (27). We suggest that this may be a result of the higher temporal resolution employed in our investigation (frame/1.16 seconds). The first peak of the cortex and OM of the right kidney was evident. In contrast, the first peak of the inner medulla was minimal or even unclear, because the blood volume of IM is considerably lower than that of the cortex and outer medulla. After the reperfusion episode, the magnitude of left cortical enhancement was slightly delayed. The first peak wash-out of the left renal cortex was slow in group 2, but disappeared in

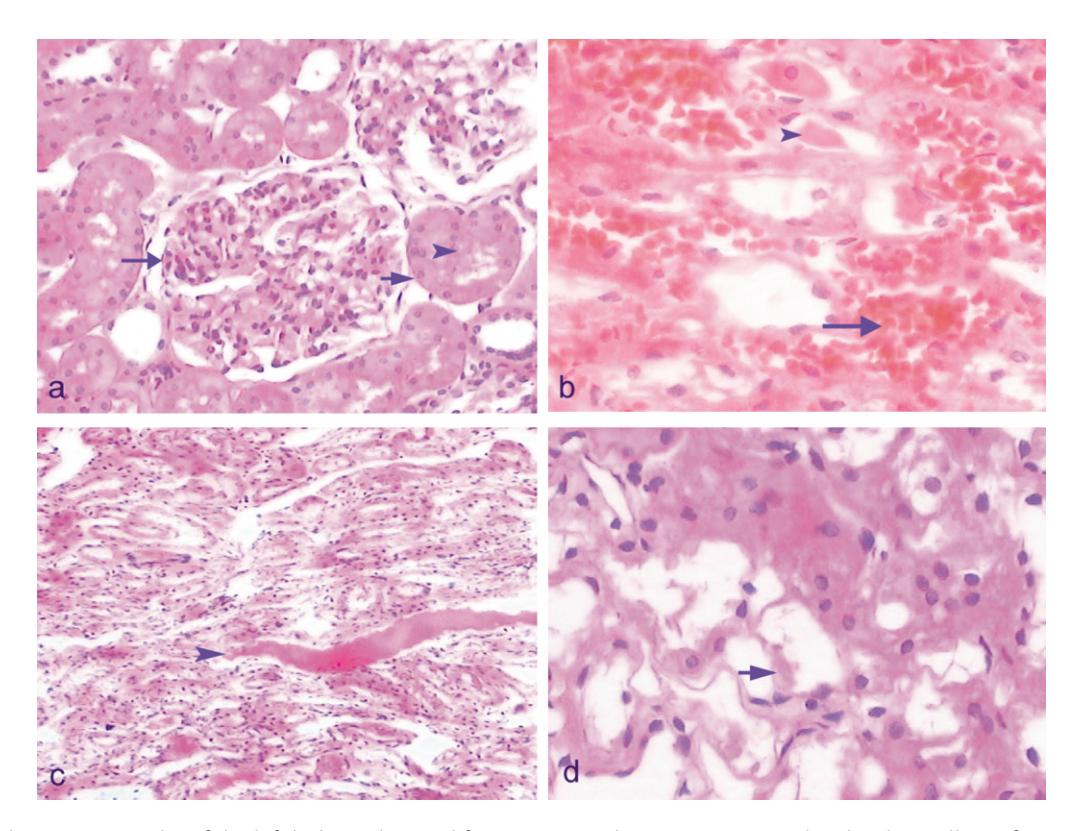


Figure 8. Photomicrography of the left kidney obtained from an animal in group 3. Note the cloudy swelling of proximal tubular endothelial cells with normal glomeruli (long and short arrows), flocculent pink protein casts in the tubular lumina (arrowhead), \times 200 (a), flocculent pink protein casts in the tubular lumina (arrowhead), hemorrhage in the interstitium and renal tubules (long arrow), \times 400 (b), tubular dilatation and protein casts in the tubular lumen (arrowhead), \times 100 (c), denuded epithelium and necrosis of tubular cells (short arrow), \times 400 (d). H&E stain.

both groups 3 and 4. The second peak of the left renal cortex was not identified in all groups. The area under the curve of the cortex was similar for groups 2, 3, and 4. We assume that the proximal convoluted tubule was damaged, but cortical blood flow was maintained despite diminished renal function, as reported previously (31,34). However, after reperfusion, the first and second peaks of OM and IM were not identified in all groups, and displayed uniphasic enhancement pattern. Moreover, the area under the curves of OM and IM was obviously reduced. The concentration function of renal tubule and collecting duct was damaged which may account for these findings. Intratubular pressure increased due to obstructing materials, epithelial edema, and intense peritubular capillary hemorrhage. As a result, the glomerular ability to filter Gd-DTPA decreased. A single coronal slice may present a better overall view of the kidneys.

It must be noted that the techniques used in this study have several limitations. First, although no severe motion artifacts were identified using single-shot EPI, the quality of some images was poor due to artifacts derived from susceptibility and motion. Second, we used some methods to obtain consistent SI measurements, but could not completely exclude inconsistencies due to free breathing. Further validation studies are required with the use of more accurate measurement. Third, renal volume in post-occlusion was slightly smaller than that in pre-occlusion due to blood inflow stop, which may have influenced the accuracy of SI measurements. Finally, we did not monitor blood pressure during our experiments. Renal arterial occlusion may lead to transient blood pressure elevation. Again, prolonged anesthesia may cause hypotension, which exacerbates the effects of ischemia. These factors may limit the use of the right kidney as a control.

In conclusion, it is possible to perform a comprehensive evaluation of renal function of dog kidney following normothermic ischemia and reperfusion injury using a combination of MR DWI and first-pass perfusion imaging. Our MR study indicates that damage to the OM and IM layer may be a primary effect of this episode, which correlates with histological findings. Our results provide a useful insight into transplantation research. However, further studies are needed to confirm these preliminary observations for noninvasive evaluation of the graft status in patients with suspected ATN during the early post-transplant period.

ACKNOWLEDGMENTS

We thank Professor Jing Shi, Professor Yan-Gang Zhang, Guang-Hui Xu, and Mrs. Ying Che for help with animal surgical procedures, and Professor Yan-Feng Zhong, Professor Hong-Bin Han, and Professor Jian-Yu Liu for their invaluable assistance.

REFERENCES

- Lechevallier E, Dussol B, Luccioni A, et al. Posttransplantation acute tubular necrosis: risk factors and implications for graft survival. Am J Kidney Dis 1998;32:984–991.
- 2. Brown ED, Chen MY, Wolfman NT, Ott DJ, Watson Jr NE. Complications of renal transplantation: evaluation with US and radionuclide imaging. Radiographics 2000;20:607–622.

Szolar DH, Preidler K, Ebner F, et al. Functional magnetic resonance imaging of human renal allografts during the post-transplant period: preliminary observations. Magn Reson Imaging 1997; 15:727–735.

- Keogan MT, Edelman RR. Technologic advances in abdominal MR imaging. Radiology 2001;220:310–320.
- Prasad PV, Priatna A. Functional imaging of the kidneys with fast MRI techniques. Eur J Radiol 1999;29:133–148.
- Powers TA, Lorenz CH, Holburn GE, Price RR. Renal artery stenosis: in vivo perfusion MR imaging. Radiology 1991;178:543–548.
- Pickens 3rd DR, Jolgren DL, Lorenz CH, Creasy JL, Price RR. Magnetic resonance perfusion/diffusion imaging of the excised dog kidney. Invest Radiol 1992;27:287–292.
- Müller MF, Prasad PV, Bimmler D, Kaiser A, Edelman RR. Functional imaging of the kidney by means of measurement of the apparent diffusion coefficient. Radiology 1994;193:711–715.
- Siegel CL, Aisen AM, Ellis JH, Londy F, Chenevert TL. Feasibility of MR diffusion studies in the kidney. J Magn Reson Imaging 1995;5: 617–620.
- Vexler VS, Roberts TP, Rosenau W. Early detection of acute tubular injury with diffusion-weighted magnetic resonance imaging in a rat model of myohemoglobinuric acute renal failure. Ren Fail 1996;18: 41–57
- Namimoto T, Yamashita Y, Mitsuzaki K, Nakayama Y, Tang Y, Takahashi M. Measurement of the apparent diffusion coefficient in diffuse renal disease by diffusion-weighted echo-planar MR imaging. J Magn Reson Imaging 1999;9:832–837.
- Fukuda Y, Ohashi I, Hanafusa K, et al. Anisotropic diffusion in kidney: apparent diffusion coefficient measurements for clinical use. J Magn Reson Imaging 2000;11:156–160.
- Choyke PL, Frank JA, Girton ME, et al. Dynamic Gd-DTPA-enhanced MR imaging of the kidney: experimental results. Radiology 1989;170:713–720.
- Carvlin MJ, Arger PH, Kundel HL, et al. Use of Gd- DTPA and fast gradient-echo and spin-echo MR imaging to demonstrate renal function in the rabbit. Radiology 1989;170:705–711.
- Frank JA, Choyke PL, Girton ME, et al. Gadolinium-DTPA enhanced dynamic MR imaging in the evaluation of cisplatinum nephrotoxicity. J Comput Assist Tomogr 1989;13:448–459.
- Semelka RC, Hricak H, Tomei E, Floth A, Stoller M. Obstructive nephropathy: evaluation with dynamic Gd-DTPA-enhanced MR imaging. Radiology 1990;175:797–803.
- Laissy JP, Faraggi M, Lebtahi R, et al. Functional evaluation of normal and ischemic kidney by means of gadolinium-DOTA enhanced TurboFLASH MR imaging: a preliminary comparison with 99Tc-MAG3 dynamic scintigraphy. Magn Reson Imaging 1994;12: 413–419.
- Grenier N, Trillaud H, Combe C, et al. Diagnosis of renovascular hypertension: feasibility of captopril-sensitized dynamic MR imaging and comparison with captopril scintigraphy. Am J Roentgenol 1996;166:835–843.
- Taylor J, Summers PE, Keevil SF, et al. Magnetic resonance renography: optimisation of pulse sequence parameters and Gd-DTPA dose, and comparison with radionuclide renography. Magn Reson Imaging 1997;15:637–649.
- Vosshenrich R, Kallerhoff M, Grone HJ, et al. Detection of renal ischemic lesions using Gd-DTPA enhanced turbo FLASH MRI: experimental and clinical results. J Comput Assist Tomogr 1996;20: 236-243.
- Dalla-Palma L, Panzetta G, Pozzi-Mucelli RS, Galli G, Cova M, Meduris S. Dynamic magnetic imaging in the assessment of chronic medical nephropathies with impaired renal function. Eur Radiol 2000;10:280–286.
- Mostafavi MR, Chavez DR, Cannillo J, Saltzman B, Prasad PV. Redistribution of renal blood flow after SWL evaluated by Gd-DTPAenhanced magnetic resonance imaging. J Endourol 1998;12:9–12.
- 23. Sharma RK, Gupta RK, Poptani H, Pandey CM, Gujral RB, Bhandari M. The magnetic resonance renogram in renal transplant evaluation using dynamic contrast-enhanced MR imaging. Transplantation 1995;59:1405–1409.
- Nakashima R, Yamashita Y, Tomiguchi S, Tsuji A, Takahashi M. Functional evaluation of transplanted kidneys by Gd-DTPA enhanced turbo FLASH MR imaging. Radiat Med 1996;14:251–256.
- Preidler KW, Szolar D, Schreyer H, et al. Differentiation of delayed kidney graft function with gadolinium-DTPA-enhanced magnetic resonance imaging and Doppler ultrasound. Invest Radiol 1996;31: 364–371.

- 26. Nelson KL, Gifford LM, Lauber-Huber C, Gross CA, Lasser TA. Clinical safety of gadopentetate dimeglumine. Radiology 1995;196:439–443.
- Suga K, Ogasawara N, Okazaki H, Sasai K, Matsunaga N. Functional assessment of canine kidneys after acute vascular occlusion on Gd-DTPA-enhanced dynamic echo-planar MR imaging. Invest Radiol 2001;36:659–676.
- Yamada I, Aung W, Himeno Y, Nakagawa T, Shibuya H. Diffusion coefficients in abdominal organs and hepatic lesions: evaluation with intravoxel incoherent motion echo-planar MR imaging. Radiology 1999;210:617–623.
- 29. Best J, Lavender JP, Russell S, Sherwood T. Preservation of normal cortical vasculature in ischaemic renal failure in the dog. Nephron 1976;16:188–196.
- Roth E, Halmagyi G, Torok B. Structural changes in temporarily ischaemized and reperfused dog kidneys. Acta Chir Acad Sci Hung 1977;18:393–415.
- 31. Williams RH, Thomas CE, Navar LG, Evan AP. Hemodynamic and single nephron function during the maintenance phase of ischemic acute renal failure in the dog. Kidney Int 1981;19:503–515
- 32. Brezis M, Rosen S. Hypoxia of the renal medulla—its implications for disease. New Engl J Med 1995;332:647–655.
- 33. Frank JA, Choyke PL, Austin HA, Girton ME. Functional MR of the kidney. Magn Reson Med 1991;22:319–323.
- 34. Riley AL, Alexander EA, Migdal S, Levinsky NG. The effect of ischemia on renal blood flow in the dog. Kidney Int 1975;7:27–34.